Modelling of time resolved spectra of Light Harvesting Antenna and Photosynthetic Reaction Center

Background exercise 12

Relation to Photosynthesis & Biofuels

PCP in nature

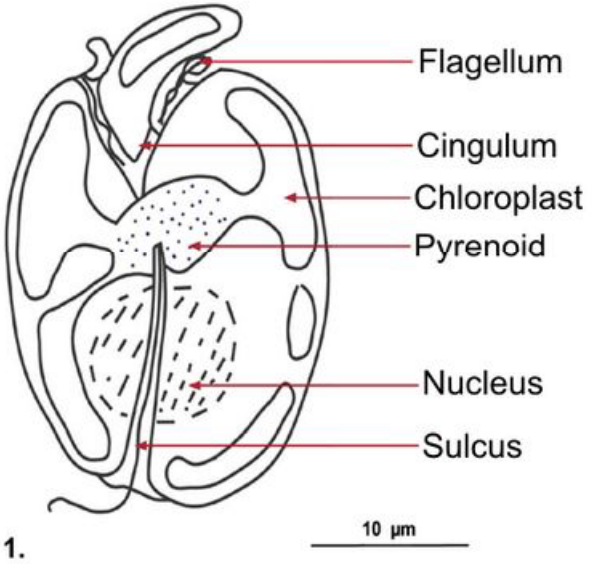

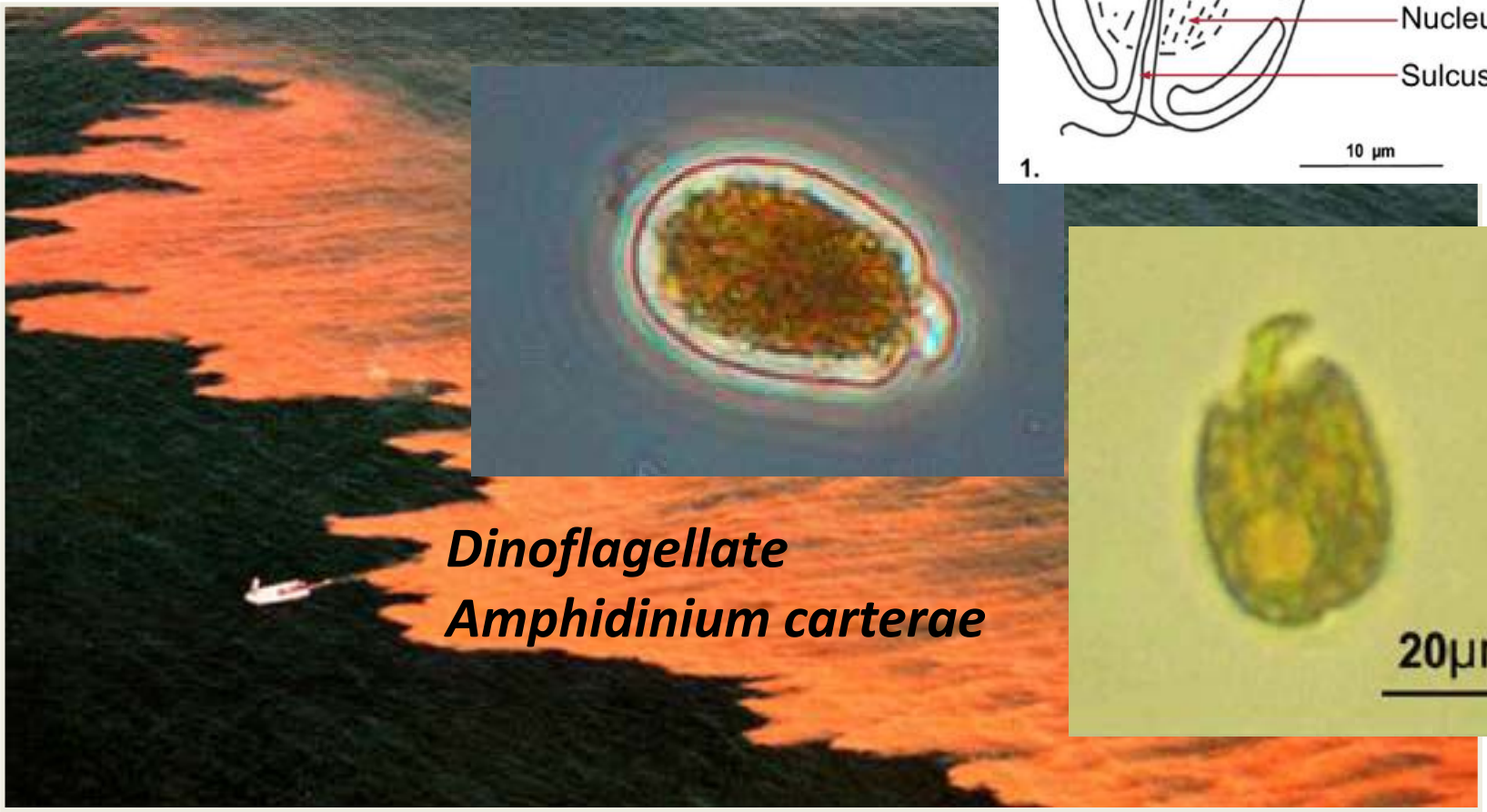

Fast Tools are Required to Study Fast Dynamics

Time Resolution is too slow to identify the motions of interest

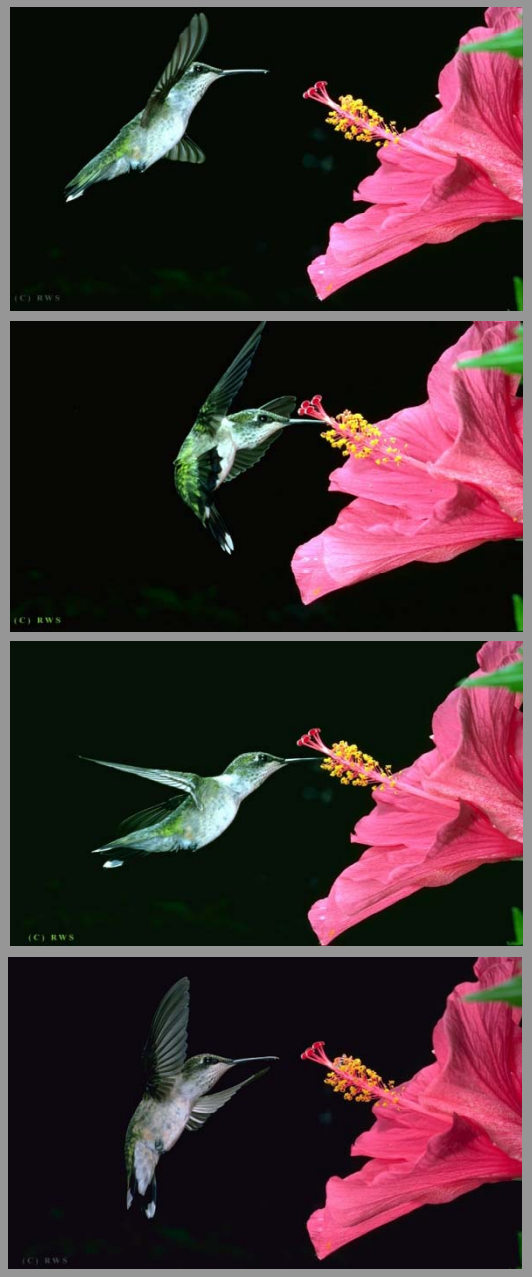

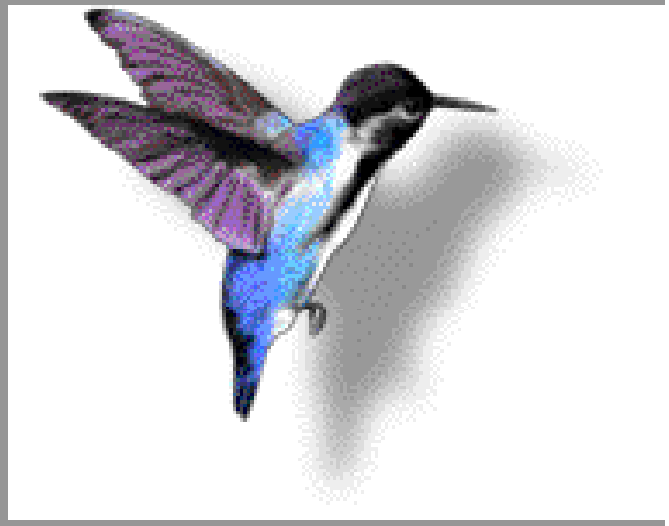

With sufficient time resolution, a detailed understanding of the fast dynamics can be extracted

Dispersed Pump-Probe

Measure the *pump-induced* absorption changes in the sample and study:

- Energy Transfer
- Reaction Dynamics
- Internal Conversion
- Intersystem Crossing
- Solvation Dynamics
- Vibrational Relaxation
- Proton Transfer
- Electron Transfer

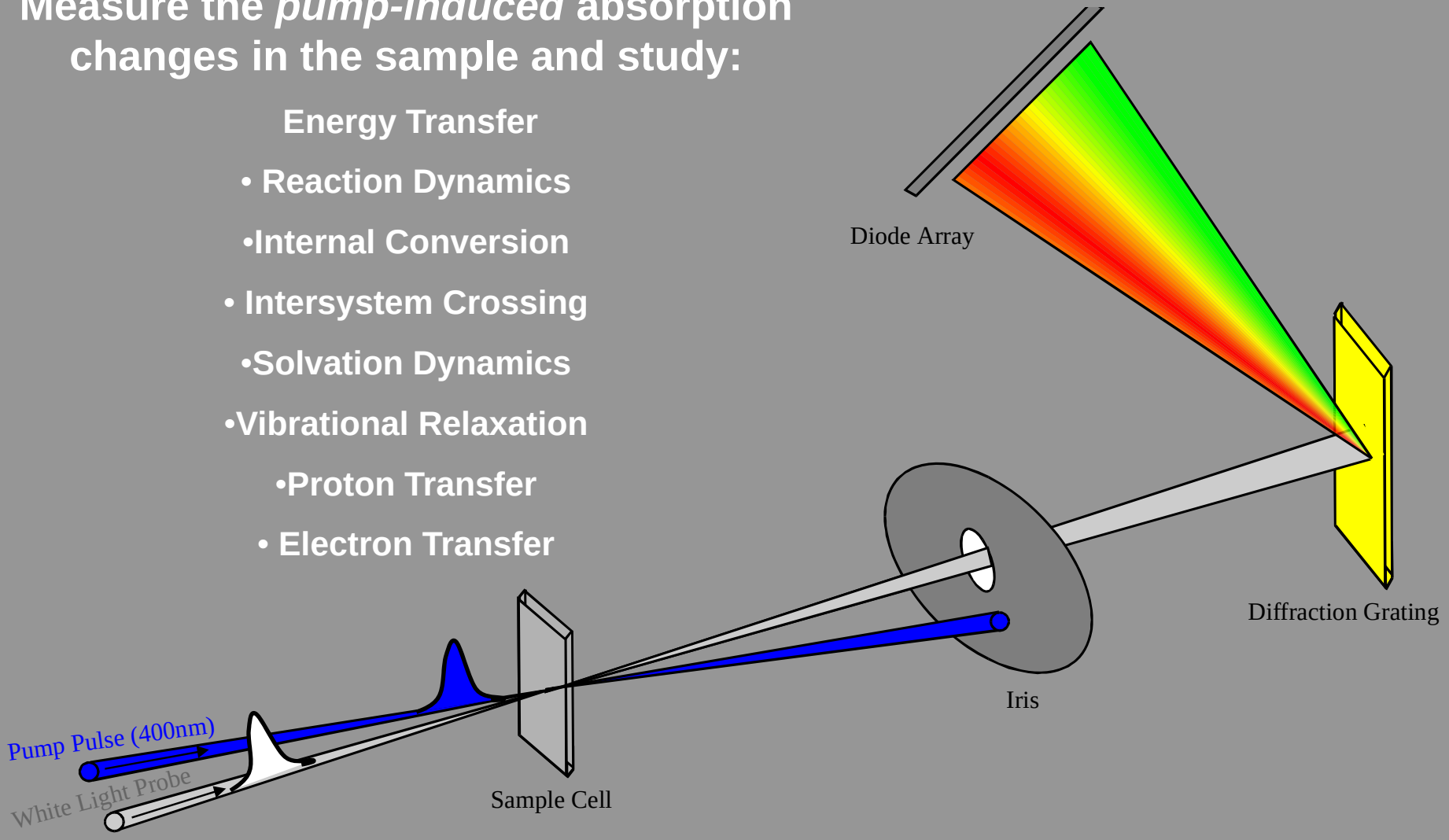

Decomposing a Transient Absorption Spectrum

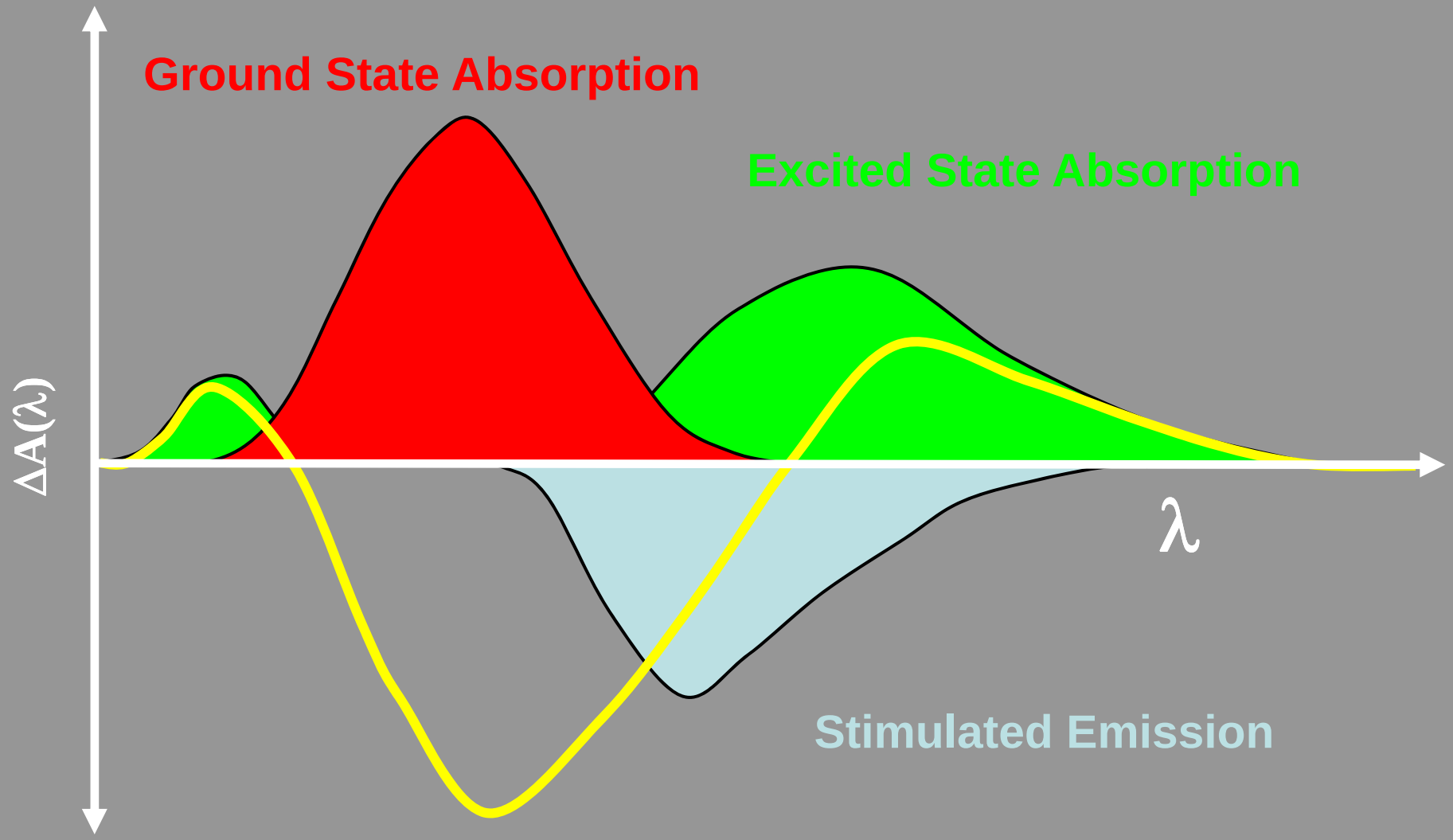

Target analysis of energy transfer and annihilation in Peridinin Chlorophyll-a Protein (PCP)

Ivo van Stokkum, Dept of Physics and Astronomy, Faculty of Sciences, VU

experiments were done at the VU by Manolis, Mikas and Delmar, and in Lund by Donatas Zigmantas and Tomas Polivka

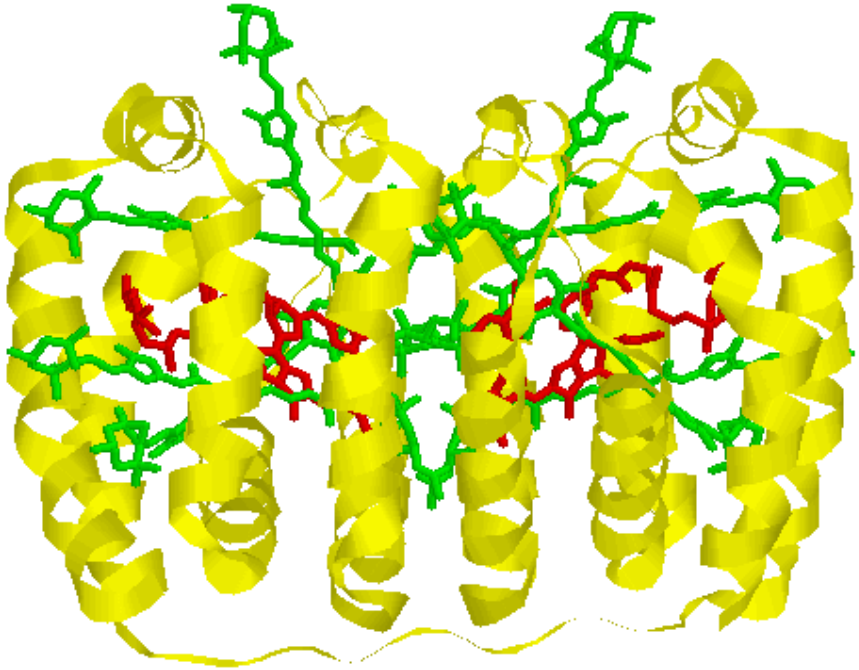

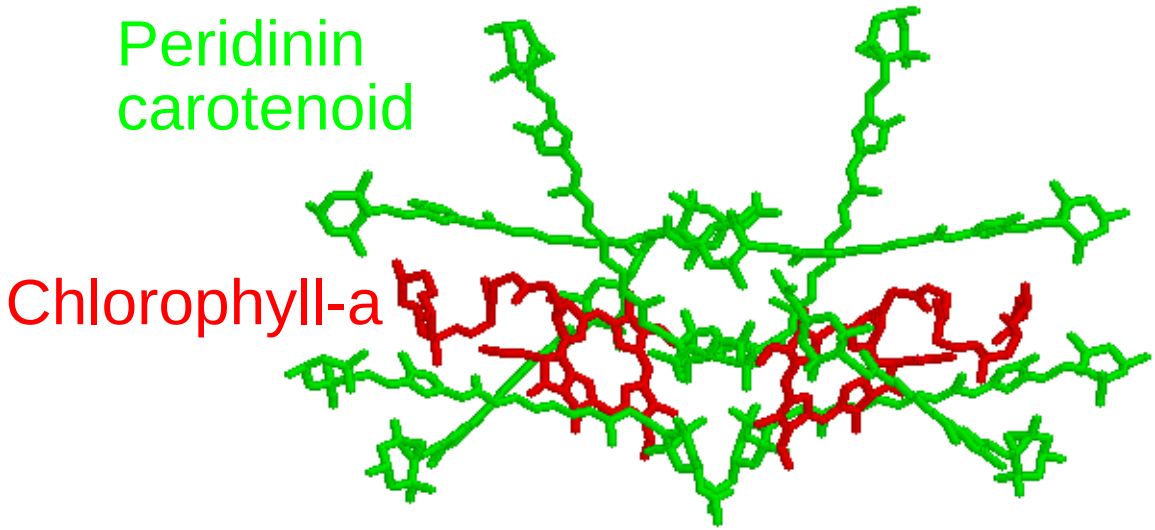

Function: light harvesting, energy transfer

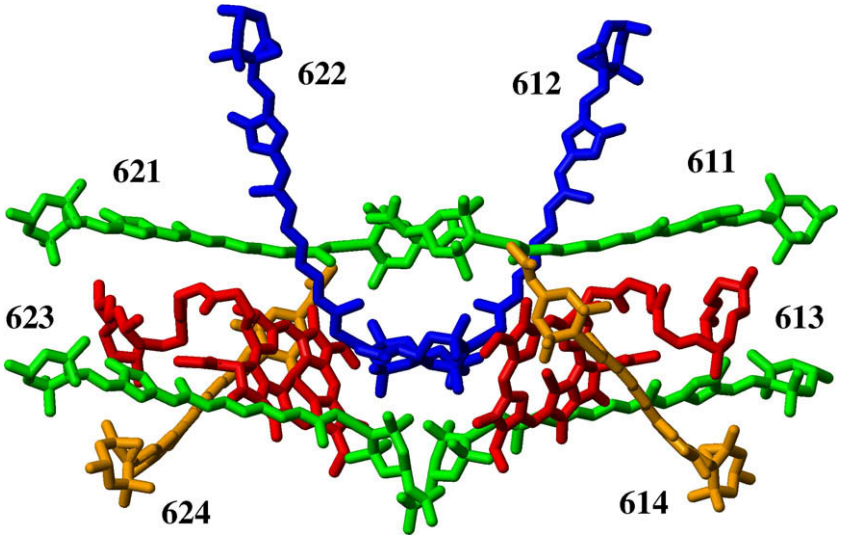

Fig. 1. Arrangement of pigments in PCP monomer. Key: peridinin (blue, green, orange), Chl-a (red). Numbers refer to the peridinin notation based on PDB entry 1PPR [3]. (For interpretation of color in this figure, the reader is referred to the web version of this article.)

contrast, the two chlorophyll molecules are not very close to each other at a distance of 17.4 Å [3].

The pigment composition and geometry in PCP is suggestive of their function; the absorption spectrum in Fig. 2 illustrates that peridinins are crucial light-harvesters, as the chlorophylls exhibit relatively weak features at 435 nm (Soret) and 670 nm (Q_y). The peridinin absorption band is intense and extends from 400 to 550 nm. This absorbance, as in all carotenoids, corresponds to the transition from the ground to the S_2 state by the absorption of one photon [27]. Studies on excitation energy transfer (EET) in PCP have shown that peridinin has an overall ≈90% efficiency of donating its singlet energy to chlorophylls [5,10]. Despite prediction from calculations that no EET proceeds from the S_2 state of peridinin [8], transient absorption experiments have demonstrated that ≈30% of the absorbed energy is transferred to chlorophylls directly from the S_2 state [6,7].

Studies of peridinin in various solvents have illustrated that, as a result of its functional groups, the singlet excited-state manifold is particularly complex; it includes an intra-molecular charge transfer (ICT) state which coexists with the "normal" S_1 state of typical carotenoids [20,21]. This ICT state, which is observed in polar (e.g. methanol) but not in non-polar solvents (e.g. hexane) is characterized by an excited-state absorption (ESA) that is red-shifted compared to that of pure S_1 as observed in hexane [20–23] and by a stimulated emission (SE) band that appears in the near infrared region [21,22]. The SE band of the ICT state was also observed in PCP, where, after the excitation of peridinin, its decay dynamics are correlated with the rise of the chlorophyll signal, leading to the conclusion that the ICT is a major energy funnel towards chlorophyll [7]. Pump-dump-probe experiments have shown that for peridinin dissolved in methanol the S_1 and the ICT states are separate entities, that equilibrate on the timescale of a few picoseconds [23,26]. In PCP, both the S_1 and ICT state are thought to participate in the EET process, which occurs on a picosecond timescale.

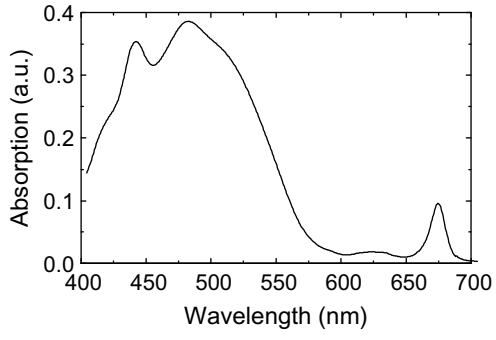

Fig. 2. Absorption spectrum of PCP.

The current study aims at characterizing the interactions between the peridinins and the chlorophylls in PCP by using ultrafast transient absorption techniques and global and target analysis methodologies. First we will address the interaction between excited peridinin molecules and the chlorophylls in PCP. We will then present a target analysis model that captures the essence of the peridinin-to-chlorophyll energy transfer processes in PCP and describes the spectral and temporal properties of the involved states. This model will also be tested with low temperature data. In the second part, we will present and discuss the results of a multi-pump transient absorption experiment, where a 500-nm pulse is used to excite peridinins while the chlorophylls in PCP have been pre-excited by a 400-nm pulse and are in their excited state. Finally, we directly excite the chlorophylls in PCP and address their interaction with the ground-state peridinins, which allows us to identify the interaction between the chlorophyll and a specific peridinin.

2. Materials and methods

2.1. Sample preparation

PCP complexes from *A. carterae*, isolated as described earlier [2], were dissolved in an aqueous buffer with 25 mM TRIS, 2 mM KCl and a pH of 7.5. At the concentrations used PCP will be mostly in its trimeric form.

2.2. Transient absorption spectroscopy

Ultrafast transient absorption measurements were performed with a set-up described in detail earlier [28,29]. The basis of the system is a 1-kHz amplified Ti:Sapphire system (Coherent-BMi α1000) delivering 450-μJ, 60-fs, 800-nm pulses. Part of the output of the amplifier was used to pump a homemade non-collinear optical parametric amplifier (NOPA) which generates visible pulses that can be tuned for selective pigment excitation. For the

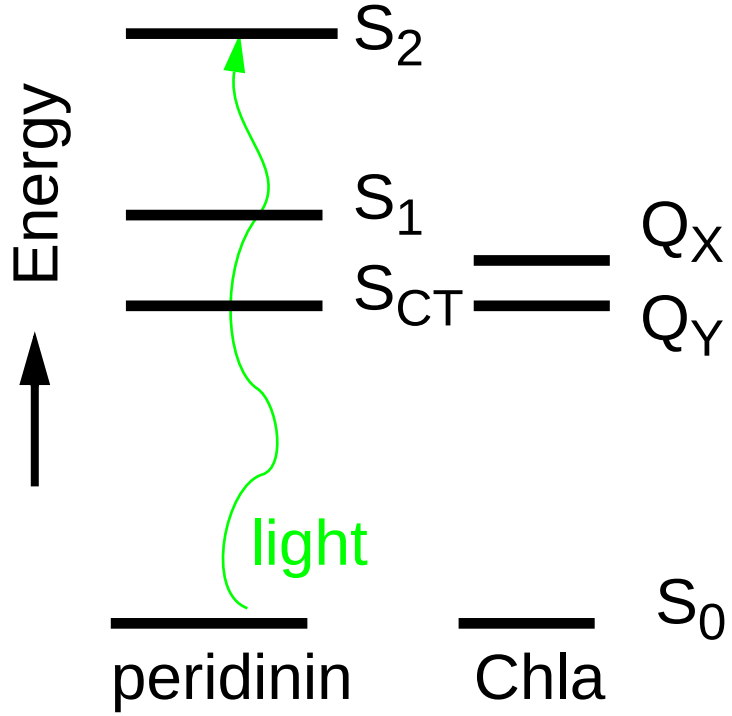

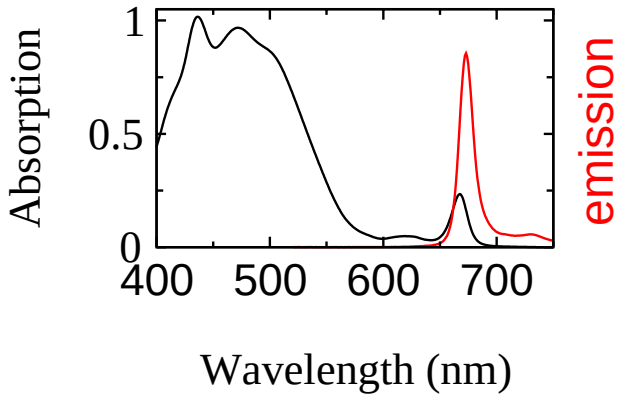

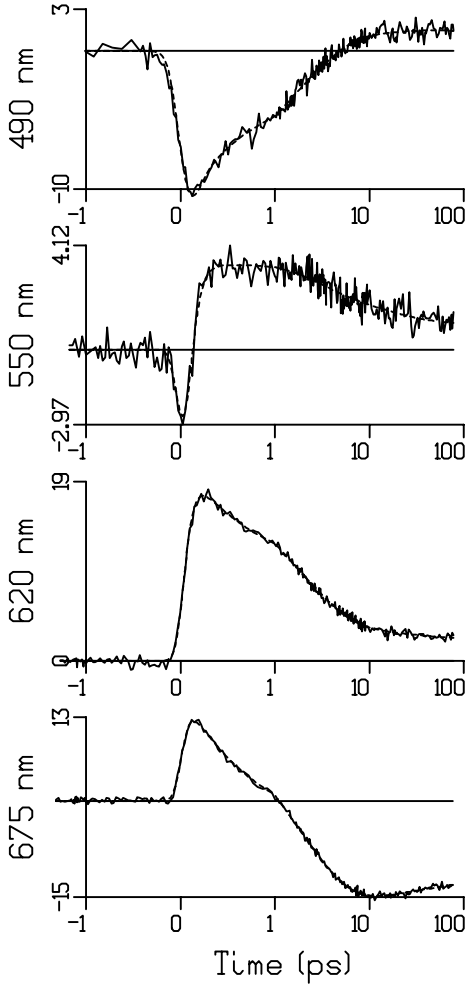

490 nm exc

ΔAbsorption
(Lund data)

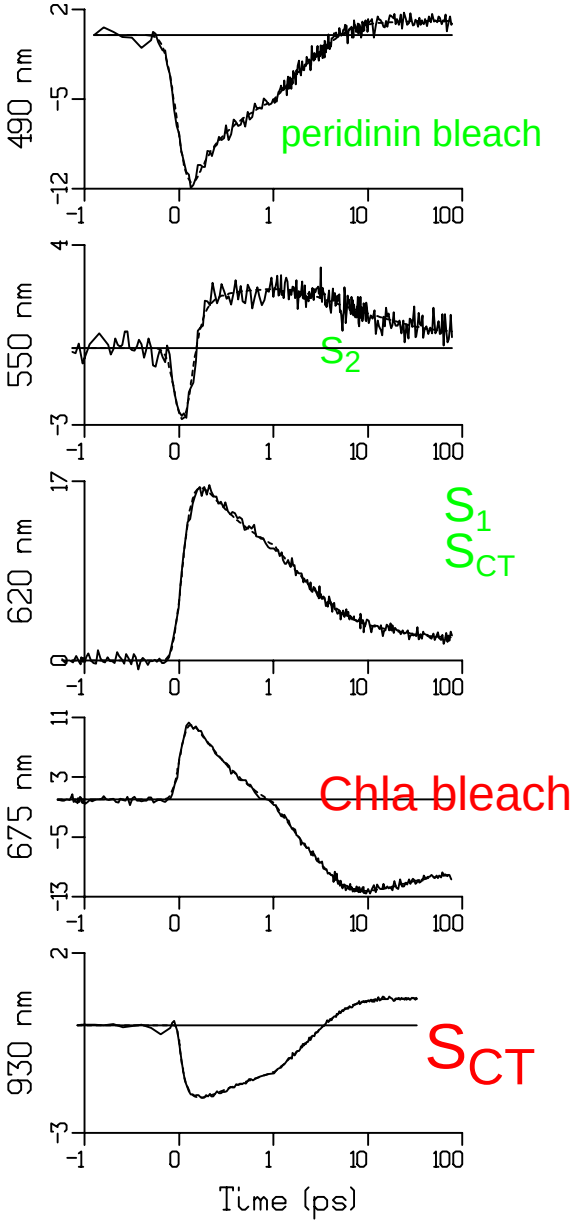

535 nm exc

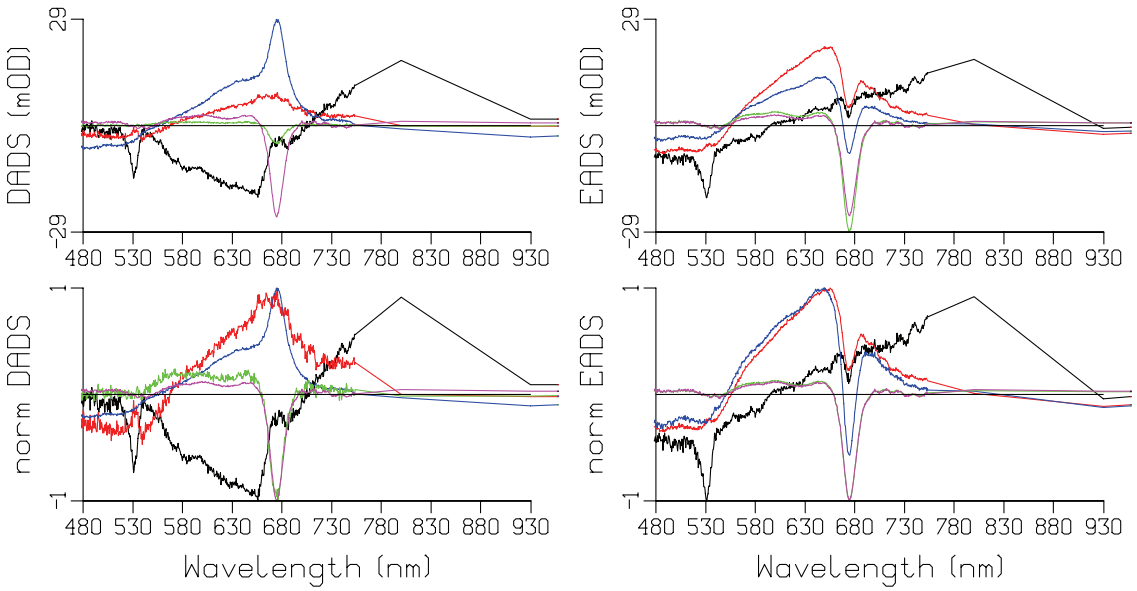

Figure S 5

Top row: DADS and EADS estimated from magic-angle pump-probe data after 535 nm excitation measured in a 72 ps time range. Bottom row shows normalized DADS and EADS. Key: 0.09 ps (black), 0.5 ps (red), 2.4 ps (blue), 20 ps (green), 2 ns fixed (magenta).

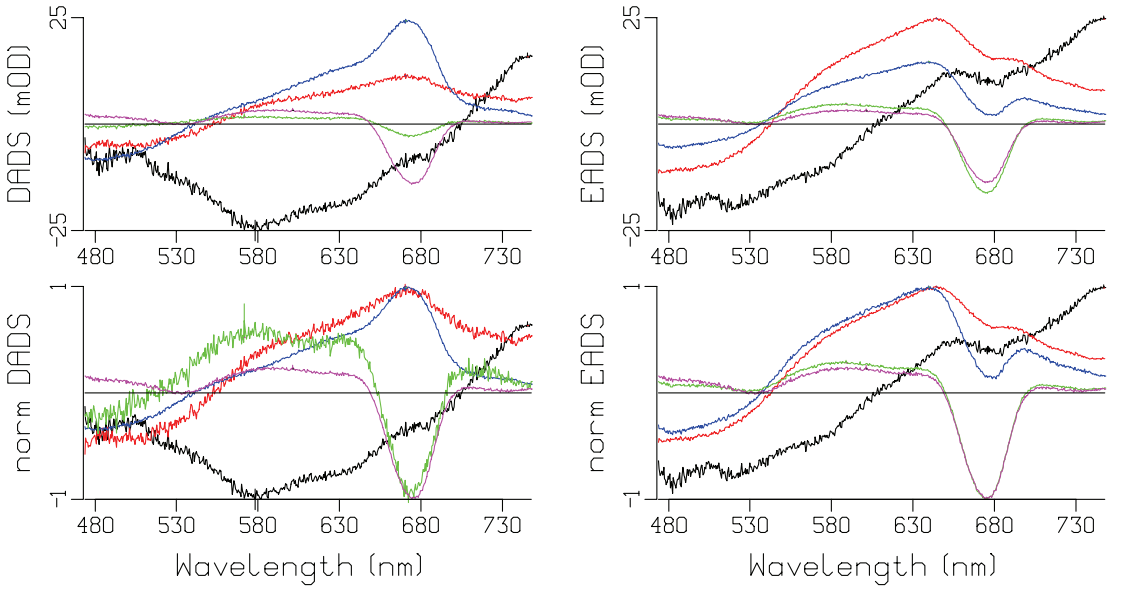

Figure S 6

Top row: DADS and EADS estimated from magic-angle pump-probe data after 490 nm excitation measured in a 72 ps time range. Bottom row shows normalized DADS and EADS. Key: 0.07 ps (black), 0.5 ps (red), 2.5 ps (blue), 21 ps (green), 2 ns fixed (magenta).

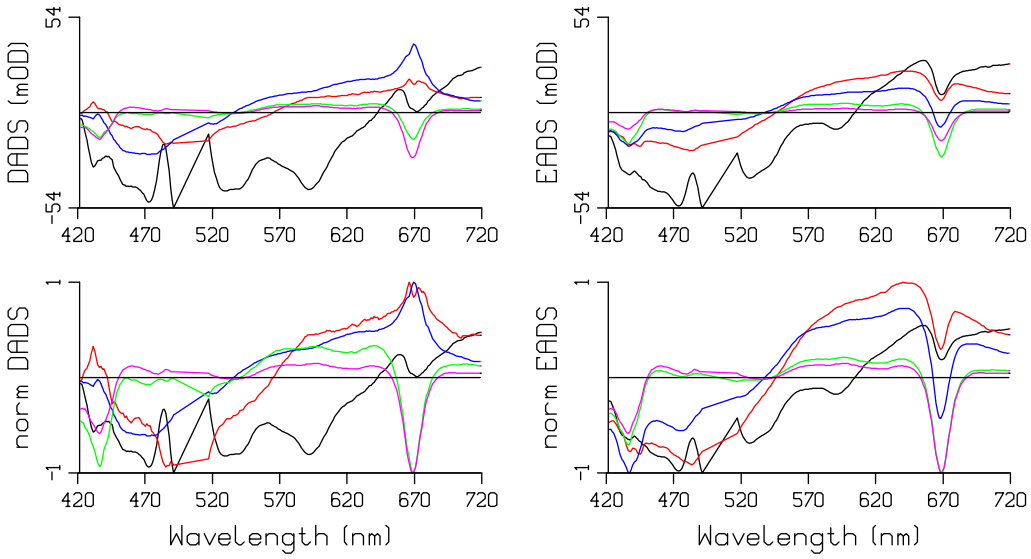

Fig. 3. Top row: DADS and EADS estimated from magic angle pump-probe data after 500 nm excitation. Bottom row shows normalized DADS and EADS. Key: 0.06 ps (black), 0.6 ps (red), 2.3 ps (blue), 33 ps (green), 1.9 ns (magenta). Note that (here and in Figs. 5 and 11) a straight line connects from 492 to 516 nm, because these data are missing. (For interpretation of color in this figure, the reader is referred to the web version of this article.)

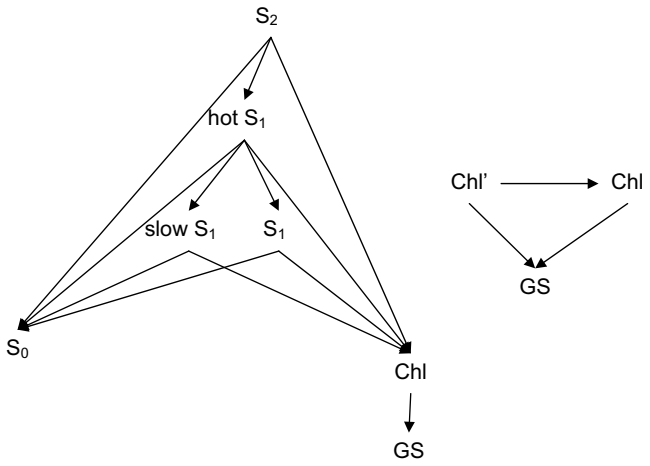

Fig. 4. Kinetic schemes used for the target analysis. Left, the channels of Per* excited-state evolution, Per* to Chl energy transfer and of Per* decay to its ground-state. Right, the scheme used to model Chl'* to Chl* annihilation. Further explanation is in text.

Table 1
Rate constants (in 1/ps) estimated from target analysis, using the kinetic schemes of Fig. 4.

From	To	Pump probe, RT	After prepump, RT	Pump probe, 77 K
S_2	Hot S_1	11	12	9.9
Hot S_1	S_1	0.6	0.6	0.6
Hot S_1	Slow S_1	0.2	0.2	0.2
S_1	Chl	0.40	0.32	0.40
Slow S_1	Chl	0.02	0.015	0.01
Chl	GS	0.0005	0.0005	0.001
S_2	Chl	4.1	2.3	5.1
Hot S_1	Chl	0.60	0.46	0.57
S_2	S_0	0.04	1.9	0.02
Hot S_1	S_0	0.04	0.2	0.02
S_1	S_0	0.04	0.13	0.02
Slow S_1	S_0	0.04	0.045	0.02
Chl′	Chl	0.019	0.015	0.057
Chl′	GS	0.013	0.017	0.032

Estimated relative error is 25%.

above. The red SADS represents hot S_1, showing broad ESA. The branching ratios from the excited Per states were adjusted to minimize the Chl Q_y features in their SADS. Thus the red, blue and green SADS are almost free from Chl Q_y features. The blue SADS represents S_1, showing a small blue shift (relative to the red SADS) of the isosbestic point. The green SADS, which represents slowly decaying S_1, shows less ESA above 600 nm. Its shape resembles more the S_1 SADS of Per as resolved from the equilibrium with ICT in methanol [23,26]. Thus its lack of ICT character might be the cause of its slow energy transfer to Chl. Other causes may be an unfavorable orientation (e.g. of the Per 612 and Per 622, cf. Fig. 1 and [8]), or less carotenoid backbone deformation. Note that from the target analysis we propose a lifetime of ≈16 ps for this slowly decaying S_1, which is largely due to a natural decay rate of 1/(25 ps), and to a smaller part due to energy transfer to Chl, with rate 1/(50 ps). The annihilation is adequately described by the 33 ps lifetime observed in the Chl* decay. With the excitation density used about 30% of the excitations are lost by annihilation. In reality the annihilation will be a multiexponential process, with a distribution of rates corresponding to different numbers of hops between Chl within and between trimers [13,36].

3.2. Testing the kinetic scheme with 475 nm excitation data

An independent experiment with 475 nm excitation and smaller time steps and shorter time range was successfully analysed with the same target kinetic scheme. Global analysis of these data yielded five lifetimes of ≈0.04 ps (black), 0.6 ps (red), 2.4 ps (blue), 20 ps (green). The difference between the 20 ps lifetime and the value of 33 ps found above, is attributed to the higher excitation density used here, resulting in somewhat faster annihilation and larger signals. The final lifetime was fixed at 2 ns (magenta). The estimated DADS and EADS are shown in Fig. S2. Although the first EADS shows differences, which are attributed to the larger imprecision with this short lifetime, in general the shapes are very similar to those of Fig. 3. In particular the green DADS consists of Chl* excited-state decay caused by annihilation (as evidenced by the decay of the Chl Q_y and Soret bleaches), and slowly decaying Per*, as evidenced by the decay of ESA around 560 nm and bleach around 480 nm. Target analysis using very similar parameters resulted in the SADS of Fig. S3. Again, the red, blue and green SADS

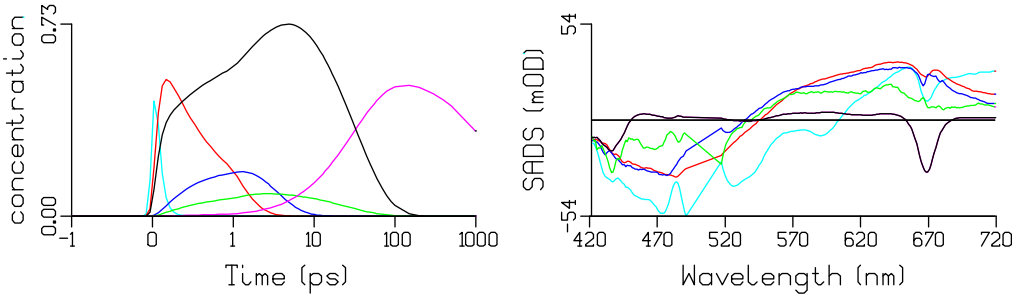

Fig. 5. Concentration profiles (left) and SADS (right) estimated from magic angle pump-probe data after 500 nm excitation using the kinetic schemes from Fig. 4. Key: S_2 (cyan), hot S_1 (red), S_1 (blue), slow S_1 (green), Chl (black), terminal Chl (magenta).

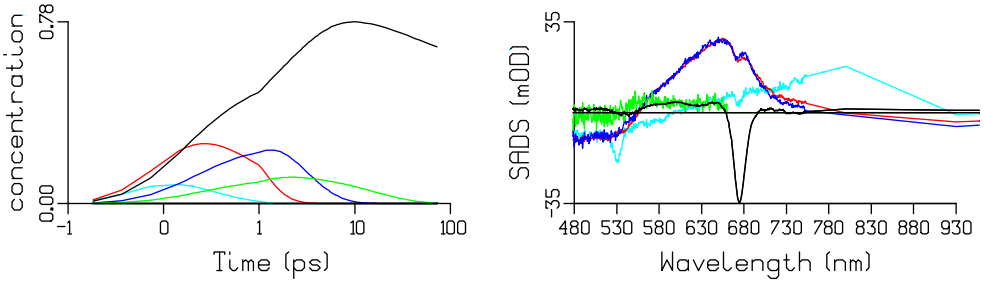

Fig. 6. Concentration profiles (left) and SADS estimated from magic angle pump-probe data after 535 nm excitation using the kinetic schemes from Fig. 4. Key: S_2 (cyan), hot S_1 (red), S_1 (blue), slow S_1 (green), Chl plus terminal Chl (black).

are almost free from Chl Q_y features. Since the SADS of the slowly decaying S_1 (green) is the smallest contribution to the data, hidden under the contributions of the other states, it is estimated less precisely than the others. Note that it is qualitatively very similar to that in Fig. 5, which corroborates our findings from the 500 nm excitation data.

3.3. Testing the kinetic scheme with visible and near IR data from [7].

The PCP model system and its components have been comprehensively studied in Sundström's laboratory in Lund. Here we apply our global and target analysis methods to measurements after 535 nm excitation in the visible and near IR as obtained by Zigmantas et al. [7], shown in Fig. S4. Most important is the 930 nm trace, which shows the decay of the stimulated emission from the Per S_1/ICT state, and rise towards the level of Chl ESA. Global analysis of these data yielded five lifetimes of ≈0.09 ps (black), 0.5 ps (red), 2.4 ps (blue), 20 ps (green). The final lifetime was fixed at 2 ns (magenta). The estimated DADS and EADS are shown in Fig. S5. Clearly both the red and blue EADS have negative amplitude at 930 nm. The green DADS consists of Chl* excited-state decay caused by annihilation (as evidenced by the decay of the Chl Q_y bleach), and slowly decaying Per*, as evidenced by the decay of ESA around 560 nm and bleach around 480 nm. But in contrast to the previous excitation wavelengths, the difference between the normalized green and magenta DADS is smaller. This indicates a smaller amount of slowly decaying S_1 in these 535 nm excitation measurements. Target analysis resulted in the SADS of Fig. 6. The green SADS has now become very small and noisy, and we assumed it to be zero above 650 nm. It does contain ESA around 560 nm and bleach around 480 nm. Again, the red and blue SADS are almost free from Chl Q_y features. Both show stimulated emission at 930 nm, indicating that both hot S_1 and S_1 are strongly coupled to the ICT state. Apparently, after 535 nm excitation only a small fraction (5–10%) of slowly decaying Per is present. In contrast, 490 nm excitation data from [7] are very comparable to the 500 and 475 nm data presented above. The estimated DADS and EADS in Fig. S6 show a clear Per* contribution in the normalized green DADS. Target analysis results of these 490 nm excitation data are depicted in Fig. 7. Again the green SADS shows a clear Per bleach, consistent with a 25% fraction of slowly decaying Per, and the ESA lacks ICT features. We propose that the slowly decaying

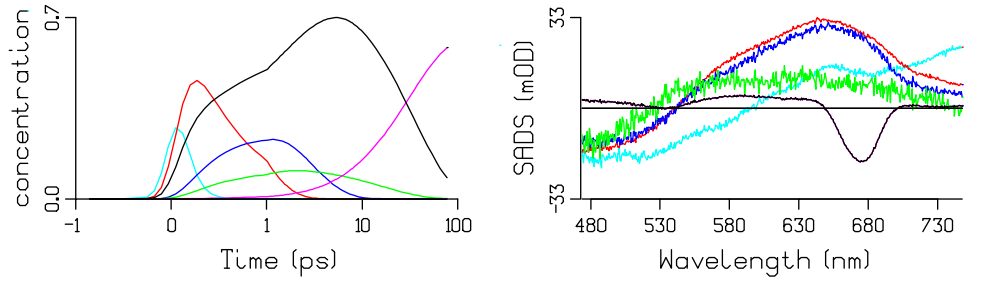

Fig. 7. Concentration profiles (left) and SADS estimated from magic angle pump-probe data after 490 nm excitation using the kinetic schemes from Fig. 4. Key: S_2 (cyan), hot S_1 (red), S_1 (blue), slow S_1 (green), Chl (black), terminal Chl (magenta). (For interpretation of color in this figure, the reader is referred to the web version of this article.)